Research Article

Journal of Physical Organic Chemistry

Received: 25 August 2007, Revised: 18 December 2007, Accepted: 23 January 2008, Published online in Wiley InterScience: 2008

(www.interscience.wiley.com) DOI 10.1002/poc.1349

Spectroscopic study of mono- and bis(styryl) dyes of the pyridinium series containing azathiacrown ether residue

E. V. Tulyakova[a]*, O. A. Fedorova[a], Yu. V. Fedorov[b], G. Jonusauskas[c] and A. V. Anisimov[a]

Phenylazathiacrown ether monostyryl and bis(styryl) dyes were synthesized and their complex forming ability was evaluated in acetonitrile by absorption and fluorescence spectroscopy. It was found that dyes are sensitive to the presence of H^+ and Hg^{2+}, Ag^+, Cu^{2+} cations. The most stable complexes were formed with mercury. Stability constants and UV–Vis spectra of complexes defined stoichiometry were determined with the use of HYPERQUAD program. Evidence was given for the occurrence of two stoichiometries: LM and LM_2. The pronounced optical response on complex formation was found both in absorption and emission spectra that could be used for optical detection of cations. Copyright © 2008 John Wiley & Sons, Ltd.

Supplementary electronic material for this paper is available in Wiley InterScience at http://www.mrw.interscience.wiley.com/suppmat/0894-3230/suppmat/

Keywords: bis(crown ether); bis(styryl)pyridinium perchlorate; phenylazathia-15-crown-5; complex formation; heavy metal cations; UV–Visible spectroscopy; fluorescence

INTRODUCTION

Topology of macrocyclic polyethers strongly contributes to their cation complexation.[1] Replacement of monocyclic crown ethers by bicyclic structures is an attractive strategy to enhance cation binding ability and selectivity of crown ethers. Macrobicyclic polyethers carrying two crown ether moieties at the end of a spacer possess interesting complexing properties.[2] It is typical for these bis(crown ethers) to form intramolecular sandwich-type complexes with metal cations bigger than crown ether cavity by means of a cooperative action of two adjacent crown ether rings. As a result of such a complex formation, the bis(crown ether) exhibits excellent selectivity towards certain cations as compared to the corresponding monocyclic analogues.[3,4] Bis(crown ethers) have also been used as cations carriers in transport experiments, giving rise to different selectivity and efficiencies.[5,6]

Bis(crown ether) derivatives are known to adsorb onto metallic surfaces and on nanoparticles, where they keep their binding properties.[7–9] In another area, the introduction of bis(crown ether) dyes into organized media has just begun, but seems promising. For example, it has been shown that triazolehemiporphyrazines, with two crown ethers and two fatty chains, can organize into Langmuir–Blodgett films.[10,11] The interaction with ions has not been studied yet, but this type of assembly could be a first step towards ionic channels in this medium. Xu's team reported a series of bis(benzocrown ether)-substituted cyanine dyes, which act as sensitizers in photographic materials.[12–16] Their sensitivity and storage ability were high as compared to that of conventional cyanine dyes. As a matter of fact, there is no doubt that bis(crown ether) dyes will lead to very interesting applications in the close future.

These considerations prompted us to conceive and study an original bis(crown ether) optical ionophores based on the mono- and bis(styryl) pyridinium derivatives. We developed the bis(crown ether) derivatives of unsymmetrical and symmetrical structures, in which two crown-containing styryl residues are conjugated with each other through the pyridinium fragment. The azathiacrown ether ionophore was chosen because of selectivity to practically important cations (Ag^+, Hg^{2+}, Cu^{2+}, Pb^{2+}).[18] Moreover, the mono styrylic dyes of this series showed interesting spectral properties. Only a few papers on bis(crown ethers) containing N, *O*-heteroatoms in crown ether moiety have been published.[17,19–25] The bis(crown ethers) with azathiacrown ether moieties have been synthesized and studied for the first time (Scheme 1).

* *Department of Chemistry, M. V. Lomonosov Moscow State University, Leninskie Hills 1/3, GSP-2, 119992 Moscow, Russia. E-mail: tulyakova@petrol.chem.msu.ru"*

a *E. V. Tulyakova, O. A. Fedorova, A. V. Anisimov*
Department of Chemistry, M. V. Lomonosov Moscow State University, Leninskie Hills 1/3, GSP-2, 119992 Moscow, Russia

b *Y. V. Fedorov*
A. N. Nesmeyanov Institute of Organoelement Compounds Russian Academy of Sciences, Vavilova str. 28, 119991 Moscow, Russia

c *G. Jonusauskas*
Centre de Physique Moléculaire Optique et Hertzienne (CPMOH), UMR 5798, Université Bordeaux 1, 351 Cours de la Libération, 33405 Talence, France

Journal of Physical Organic Chemistry

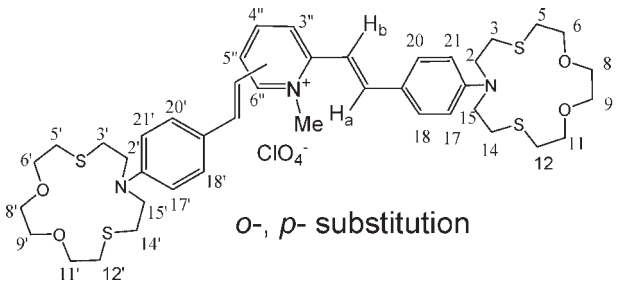

Scheme 1.

RESULTS AND DISCUSSION

Synthesis

Compounds **1–4** were synthesized by condensation reaction of crown-5-ether containing benzaldehyde with tosylates of bis- or trismethyl pyridinium in the presence of pyrrolidine in *n*-butanol using the method described by Kipriyanov.[26] Tosylates of mono- and bis(styryl)pyridinium were converted to the perchlorates (as shown in Scheme 2).

The structure of the obtained compounds was proved by combination of NMR-spectroscopy, ESI-MASS spectrometry as well as elemental analysis. According to NMR observation, all compounds were prepared as an *E*-isomer. Couple constant for the olefinic C=C protons for **1–4** are $^3J_{H,H} = 16.3$, 15.8, 15.7 and 16.2, 15.7 Hz, respectively. The difference in chemical shifts found for proton signals C(18)—H and C(18′)—H, C(20)—H and C(20′)—H, C(a)—H and C(a′)—H, C(b)—H and C(b′)—H in molecule **3** points out the unsymmetrical structure.

Steady-state absorption and emission of the dyes

Electronic absorption spectra

The electronic absorption spectra of **1–4** in CH_3CN are characterized by an intense long wavelength absorption bands (LAB) with λ_{max} in visible spectral region (Fig. 1a, Table 1). The more extensive conjugation in *p*-substituted **1** shifts its LAB bathochromically relative to that of the *o*-substituted analogue **2**. LAB of bischromophoric dyes **3** and **4** are shifted bathochromically relative to that of monochromophoric dyes **1** and **2**, due to adiabatic interaction of two ICT states in system of donor–acceptor–donor. Such shifts for bis(chromophoric) compounds have been reported previously.[21] LAB of dye **3** has an asymmetrical shape and resembles a linear combination of a stronger absorption band at 502 nm and a weaker band at 454 nm. Splitting of LAB in **3** could be due to adiabatic interaction of two non-equivalent ICT states with different positions of donor.[26–28] The molar absorptivities of **3** and **4** are higher those of **1** and **2**, due to the presence of two chromophores in **3** and **4**.

Fluorescence spectra

Fluorescence emission spectra of **1–4** recorded in acetonitrile are shown in Fig. 1b.

The fluorescence quantum yields, Φ^{fl}, of the compounds **1–4** are increased in the order **4** < **3** < **2** < **1** (Table 1). The Φ^{fl} of symmetrical *o,o*-substituted bisstyryl pyridinium dye **4** is 9.5 times lower those of asymmetrical *o,p*-substituted dye **3**, whereas

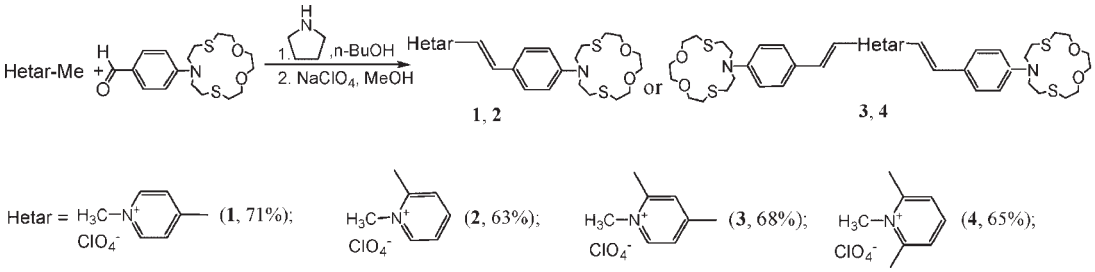

Scheme 2.

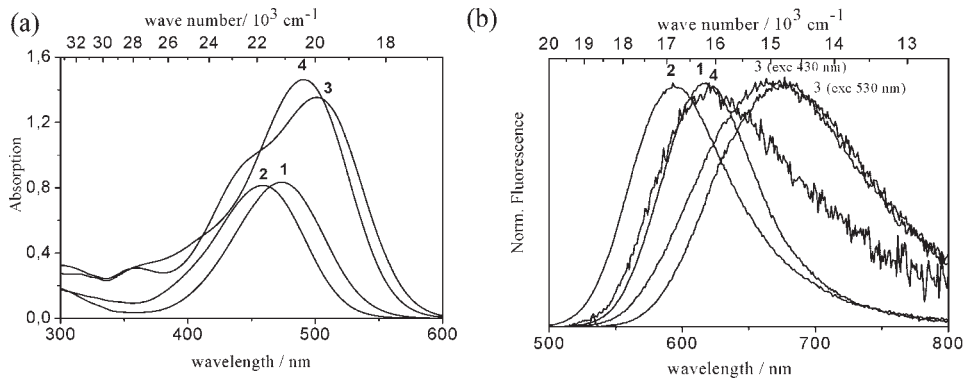

Figure 1. (a) Absorption spectra **1–4** ($c = 2.5 \times 10^{-5}$ M) in acetonitrile at 293 K. (b) Fluorescence spectra **1–4** in acetonitrile at 293 K

Table 1. Stability constants and optical properties of **1**–**4** and their complexes in acetonitrile at 293 K

Compound	ε_{trans}, 10^4 L mol^{-1} cm^{-1}	λ^{abs}_{max}, nm {$\Delta\lambda$, nm*}	Lg (K_S)	λ^{fl}_{max}, nm; ($\Delta\lambda^{fl}$, nm*)	$\Phi^{fl} \times 10^2$	Time delay, ps
1	3.48	474		618	3.0	100, 230
$(\mathbf{1})_1 \cdot (H^+)_1$		330 {144}	5.0 ± 0.1	404 {214}	0.1	n.d.($\tau < 5$)
$(\mathbf{1})_1 \cdot (Hg^{2+})_1$		350 {124}	16.5 ± 0.1	567 {51}	9.0	136, 397
$(\mathbf{1})_1 \cdot (Ag^+)_1$		440 {34}	3.91 ± 0.02	598 {20}	17	Did not measured
$(\mathbf{1})_1 \cdot (Cu^{2+})_1$		434 {40}, 780**	Not determined	567 {51}(exc440) 558 {60}(exc330)	2.1 0.8	Did not measured
2	3.25	459		593	2.7	157
$(\mathbf{2})_1 \cdot (H^+)_1$		329 {130}	5.29 ± 0.04	402 {191}	0.1	n.d.($\tau < 5$)
$(\mathbf{2})_1 \cdot (Hg^{2+})_1$		343 {116}	Not determined	548 {45}	1.3	Did not measured
$(\mathbf{2})_1 \cdot (Ag^+)_1$		423 {36}	4.42 ± 0.08	572 {21}	7.4	330
$(\mathbf{2})_1 \cdot (Cu^{2+})_1$		429 (30), 789**	6.9 ± 0.4	581{12}(exc 410 nm) 552 {41}(exc 330 nm)	1.0 0.4	113
3	5.41	454 (sh), 502		667(exc 430 nm) 668 (exc 530 nm)	1.9 2.0	140, 300
$(\mathbf{3})_1 \cdot (H^+)_1$		335 (sh) {119}, 491 {10}	5.7 ± 0.13	495 (exc 350 nm) 667(exc 490 nm)	0.8 1.0	61, 256
$(\mathbf{3})_1 \cdot (H^+)_2$		335 (sh) {119}, 353 {149}	9.9 ± 0.16	495 (exc 320 nm) 667(exc 360 nm)	1.6 1.8	37, 102
$(\mathbf{3})_1 \cdot (Hg^{2+})_1$		357 (sh) {97}, 488 {14}	>14	655 (exc 360 nm) 660 (exc 500 nm)	0.6 0.9	86, 830
$(\mathbf{3})_1 \cdot (Hg^{2+})_2$		357 (sh) {97}, 372 {130}	—	614 (exc 350 nm) 614 (exc 390 nm)	1.6 2.0	116, 382
$(\mathbf{3})_1 \cdot (Ag^+)_1$		—	3.54 ± 0.03	—	—	—
$(\mathbf{3})_1 \cdot (Ag^+)_2$		443 (sh) {11}, 467 {35}	6.14 ± 0.05	625 (exc 420 nm) 657 (exc 500 nm)	2.0 1.5	Did not measured
$(\mathbf{3})_1 \cdot (Cu^{2+})_1$			6.05 ± 0.13	—	—	—
$(\mathbf{3})_1 \cdot (Cu^{2+})_2$		432 {70}, 799**	11.27 ± 0.14	577 (exc 430 nm) 583 (exc 340 nm)	4.0 2.8	60, 270, 1360
4	5.85	491		620	0.2	15, 53
$(\mathbf{4})_1 \cdot (H^+)_1$		332 (sh) 483 {8}	6.4 ± 0.2	612{8}(exc 480 nm) 435{185}(exc300 nm)	0.4 0.6	16, 122
$(\mathbf{4})_1 \cdot (H^+)_2$		358 {133}	10.9 ± 0.2	446 {174}	7.9	123, 276
$(\mathbf{4})_1 \cdot (Hg^{2+})_1$		—	>14	—	—	—
$(\mathbf{4})_1 \cdot (Hg^{2+})_2$		378 {113}	>14	560 {80}	0.4	6.5, 52, 155
$(\mathbf{4})_1 \cdot (Ag^+)_1$			3.19 ± 0.06	—	—	—
$(\mathbf{4})_1 \cdot (Ag^+)_2$		450 {41}	6.54 ± 0.10	589 {31}	0.7	53, 350
$(\mathbf{4})_1 \cdot (Cu^{2+})_1$		433 {58}	7.5 ± 0.3	—	—	—
$(\mathbf{4})_1 \cdot (Cu^{2+})_2$		443 {48}, 821**	13.9 ± 0.4	582 {38}	1.1	220

** Lowest energy band position.

the difference between Φ^{fl} of *o*-substituted dye **2** and *p*-substituted dye **1** is negligible. It was also observed that Φ^{fl} of asymmetrical *o*,*p*-substituted dye **3** depends on excitation wavelength.

Time-resolved emission of the dyes

Monoexponential decay kinetic was only observed for dye **2**. For dyes **1**, **3**, **4** the fluorescence decay profiles could be fitted to at least two exponentials. Short and long decay times for **4** are approximately one order of magnitude lower compared with dye **3** (Table 1). Furthermore, excitation wavelength-dependent time-resolved studies of **3** suggest that either different ground-state species are excited or that the relaxation rates depend on the nature of excited CT transfer states involved.

It is well known that there might be three different channels of TICT state formation in amino(styryl) pyridinium derivatives.[29] According to the energy barrier height and the energy of the twisted state relative to that in the Franck–Condon region, the rotation around the anilino-ethylene bond should be the easiest since there is lowest barrier to rotation in the S_1 state in solution. The rotation around the pyridyl-ethylene bond is also possible but not so favoured in solvents with high dielectric constant, and rotation of the dimethylamino group should be the most difficult also due to the reduced mobility of the donor group, that is, its bulkiness in our case. The high-energy barrier to rotation around

the central double bond in the S_1 state is consistent with the low photoisomerization yield of amino(styryl) pyridinium dyes in most of the solvents.[30]

Complex formation of 1–4 with metal cations and $HClO_4$

The addition of Ag^+, Hg^{2+}, Cu^{2+} perchlorates or $HClO_4$ to a solutions of **1**–**4** in MeCN resulted in hypsochromic shifts of the LABs and of the fluorescence bands, which are evidently due to formation of complexes of metal cations with the crown ether fragments of the molecules (Scheme 2). The LAB in **1**–**4** involves displacement of electron density from the nitrogen atom of phenylaza-dithiacrown-ether moiety to the heterocyclic moiety. Binding of cations in the crown ether moieties of **1**–**4** diminishes this effect, accounting for the hypsochromic shifts of the LAB, whose magnitude depends on the identity of the metal ion. Complexation of **1**–**4** with the doubly charged mercury cations causes larger LAB hypsochromic shifts (up to 124 nm) than complexation with the singly charged silver cations (up to 36 nm).

The equilibrium constants for complex formation of dyes **1**–**4** with Ag^+, Cu^{2+} perchlorates and $HClO_4$ were calculated from the absorption spectra of solutions at constant ligands concentration and varying cations concentrations using the HYPERQUAD programme designed for use in connection with studies of chemical equilibria in solution from data obtained on potentiometric and/or spectrophotometric titrations.

Three equilibria were studied:

$$M^{+n} + L \overset{K_{11}}{\rightleftarrows} [ML]^{+n}$$

$$M^{+n} + 2L \overset{K_{12}}{\rightleftarrows} [ML_2]^{+n}$$

$$2M^{+n} + L \overset{K_{21}}{\rightleftarrows} [M_2L]^{+2n}$$

This approach is not applicable for stability constants determination for complexes of ligands **1**–**4** with Hg^{2+} because the K values are too large. The K values can be determined in such cases by spectrophotometric titration with a solution of a competing reference ligand, L_r (3-methyl-2-[(*E*)-2-(2,3,5,6,8,9,11,12-octahydro-1,7,13,4,10-benzotrioxadithia-cyclopentadecin-15-yl)-1-ethenyl]-1,3-benzothiazol-3-ium perchlorate (CSD)), for which the stability constant with Hg^{2+} is known.[31] In this work, crown-containing styryl dye CSD was employed as L_r for dyes **1**, **3**, **4**. Specifically, the competition for Hg^{2+} ions in a solution containing L_r and **1** (L_r or L_t, respectively), is described by two equilibriums, given below:

$$Hg^{2+} + L_t \overset{K_t}{\rightleftarrows} [HgL_t]^{2+}$$

$$Hg^{2+} + L_r \overset{K_r}{\rightleftarrows} [HgL_r]^{2+}$$

where L_t is a molecule of **1**, L_c is CSD; $K_t = [L_tHg]/([Hg][L_t])$ and $K_r = [L_rHg]/([Hg][L_r])$ are the stability constants of the $(\mathbf{1} \cdot Hg^{2+})$ and $[(CSD) \cdot Hg^{2+}]$ complexes, respectively. The value of $LogK_r$ was taken equal to 15.9.[31]

It was found that dyes **1**, **2** formed only one kind of complex having 1:1 stoichiometry with Hg^{2+}, Ag^+ and H^+. A distinct isosbestic point upon spectrophotometric titration of **1**, **2** with these cations were observed, confirming only one kind of complex formation.

The distortion of an isosbestic point was observed upon spectrophotometric titration of the bis(crown ether) dyes **3**, **4**, indicating more than one type of complex formation. The spectral sets for metal cations, proton and dyes **3**, **4** are consistent with formation of two complexes having 1:1 and 1:2 stoichiometries, namely, LM^{n+} and $L(M^{n+})_2$. Structures for these complexes are proposed in Scheme 2. The derived stability constants for **1**–**4** are collected in Table 1 (Scheme 3).

The highest stability constant was found for complex of mercury cations with **2**, obviously due to formation of very strong Hg^{2+}. . .S bonds in the aza-dithiacrown cavity of **2**. Strong interaction of Hg^{2+} with S atoms of dithiacrown ethers was observed earlier.[31,32] For other dyes, the stability constants for Hg^{2+} were not determined exactly due to complexity of systems studied. Nevertheless, the stability constants of complexes with Hg^{2+} of the same order of magnitude could be expected because of the identical structure of crown-ether moieties in **1**–**4**.

Monovalent Ag^+ cations form enough stable complexes with **1**–**4**, nevertheless, these complexes are much weaker than the same complexes with bivalent Hg^{2+}. Most likely the interaction between S atoms and Ag^+ plays the most important role in the stability of complexes between **1**–**4** and silver cations. Really, no complex formation in CH_3CN was observed between $AgClO_4$ and the perchlorate of 2-{2-[4-(13-aza-1,4,7,10-tetroxa-13-cyclopentadecyl)phenyl]ethenyl}-3-ethylbenzothiazolium, (CSD2), the dye with phenyl-aza-15-crown-5 moiety.[33] Moreover, very weak complex was found between Ag^+ and phenyl-aza-15-crown-5 and only aza-15-crown-5 forms enough stable complex with Ag^+ ($LogK = 4.06$).[33] The nitrogen heteroatom in phenyl-aza-15-crown-5, and especially in CSD2, are strongly involved in the π-conjugation system of the chromophores and do not participate in complexation with Ag^+. The same effect for N atom in phenyl-aza-dithia-15-crown-5 moiety may be expected in the case of dyes **1**–**4**. So the presence of S atoms into the crown-ether moiety can be responsible for complex formation of **1**–**4** with Ag^+.

The bis(crown ether) compounds **3**, **4** form two types of complexes, namely, mono-(LM^{n+}) and bismetallic $[L(M^{2+})_2]$ (Scheme 2). The binding effectiveness for the first metal cation is higher than for the second one, which could be due to Coulomb repulsion of second cation and positively charged monocomplexes (LM^{n+}).

During the protonation of **1**–**4** in CH_3CN the proton may be expected to locate at the nitrogen atom, with the oxygen and

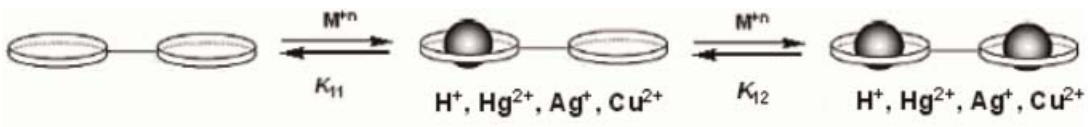

Scheme 3.

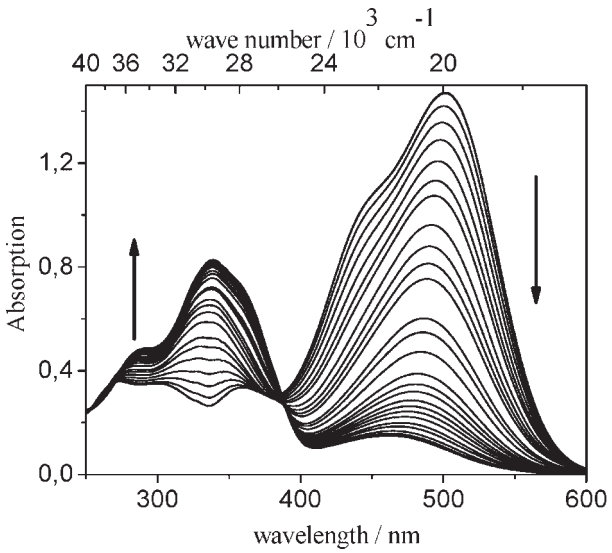

Figure 2. Spectrophotometric titration of **3** with $HClO_4$ in acetonitrile ($C_L = 2.5 \times 10^{?5}$ M, addition of $HClO_4$ $0 \leq x_{M/L} \leq 210.8$

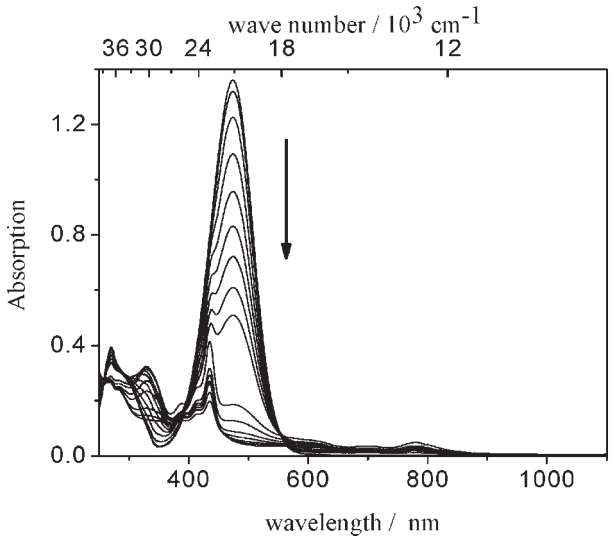

Figure 3. Spectrophotometric titration of **1** with $Cu(ClO_4)_2$ in acetonitrile ($C_L = 3.88 \times 10^{?5}$ M, addition of $Cu(ClO_4)_2$ $0 \leq x_{M/L} \leq 2.27$)

sulfur atoms within the remainder of the aza-dithia-crowns exerting only a minor influence. Such a reducing of the electron-donor strength affects strongly the absorption spectrum of the complex: the LAB moves to higher energy range (28571 cm^{-1}). The spectrophotometric titration of **3** with $HClO_4$ (Fig. 2) reveals that the addition of small amount of $HClO_4$ to **3** results in disappearance of shoulder at 454 nm originated from charge transfer from donor located at *o*-position of pyridinium ring. (The results of the spectrophotometric titration of **4** with $HClO_4$ are presented in Fig. 2a in Supporting Materials). At high concentration of acid the disappearance of the absorption band at 504 nm relevant to charge transfer from donor located at *p*-position of pyridinium ring takes place.

In conclusion, the present study reveals the values of stability constants are higher for dyes with crown ether moiety located in *o*-position of pyridinium ring than those in *p*-position. The quantum chemical calculations demonstrated that styryl fragment in *o*-position is slightly unplanned, what disturbs the conjugation between heterocyclic and crown ether parts of molecule increasing complexation ability of crown ether.

The particular changes in absorption spectra of **1**–**4** were observed upon addition of Cu^{2+} perchlorate (Fig. 3, also Figs. 3a–c in Supporting Materials). While the intensity of the lowest energy bands at 460–500 nm was drastically reduced upon addition of Cu^{2+}, at least three new spectral features appear in UV–Vis near IR spectral ranges. (1) The intraligand charge transfer band (ILCT) increases at approximately 350 nm. (2) A metal to ligand charge transfer (MLCT) band located at 400–450 nm and (3) $\sigma(S) \rightarrow Cu^{2+}$ ligand to metal charge transfer (LMCT) band as well as probably superimposed $\pi(S) \rightarrow Cu^{2+}$ LMCT and/or Cu^{2+} d–d* transition in the spectral range 500–1100 nm (ε up to 4×10^3 L mol^{-1} cm^{-1}), similar to that observed to blue copper proteins.[34,35]

It is worth to note that once complexes with Cu^{2+} have been formed, they undergo slow (few hours) changes due to oxidation–reduction intracomplex reaction which leads to reduction of Cu^{2+} to Cu^{+}. These changes accompanied with increasing the intensity of ILCT band at 350 nm, decreasing of MLCT band intensity at 400–450 nm and complete disappearance of LMCT bands at 500–1100 nm range.[35–39]

Fluorescence study of complexes of 1–4

As follows from Table 1, the blue shift of fluorescence was observed on complex formation of **1**–**4** with all cations studied and the most pronounced changes were found for proton. The changes in fluorescence quantum yields upon complex formation comprise fluorescence quenching (for **2** and **3**) as well as fluorescence enhancement (for **1** and **4**). The most probably, comparatively small changes in the relative energetic positions of emissive or non-emissive states in the excited complexes compared to each other and compared to the excited free dyes seem to be responsible for the delicate fluorescence enhancement or quenching.[40,41] The complexation of **1**–**4** obviously influences the relaxation rates (Table 1) of the excited states corresponding to subtle interplay between relaxation involving formation of twisted states and *E*–*Z*-isomerization processes.

As we can reasonably suppose, the relaxation of exited state of pure ligands goes mainly through the formation of twisted states with further non-radiative relaxation to the ground state via 'loose bolt' mechanism.[42]

The protonation of monostyryl dyes **1**, **2** shifts their LABs to higher energy region due to much weaker ICT. The later strongly reduces the possibility to form twisted states, thus the principle relaxation channel becomes *E*–*Z*-photoisomerization. Yet, in bisstyryl dyes **3**, **4**, it could be proposed that the electron acceptor could be extended to the ethylene fragment of the adjacent styryl with respect to the dimethyl-amino-styryl donor group of the dye. When ICT take place, probably, a twisting of single bond of extended acceptor could fix the excited state hindering isomerization process as compared with monostyryl dyes. This possibly could lead to the spectacular enhancement of the fluorescence quantum yield in case of complex $(\mathbf{4})_1 \cdot (H^+)_2$.

As we have not detected any fluorescence band shifts in time, we suppose that in the excited states only one state is emissive and most probably it is a relaxed locally excited state with planar

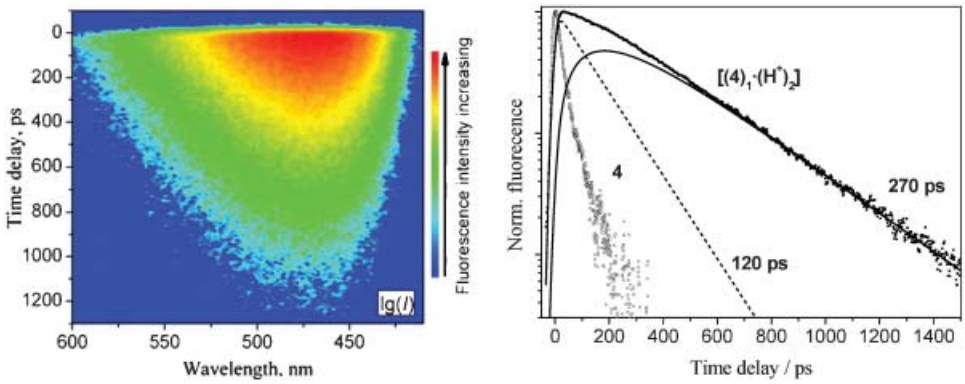

Figure 4. Time-spectrum-resolved fluorescence map (left) and fluorescence decay curves of free ligand **4** and its complex $(\mathbf{4})_1 \cdot (H^+)_2$ in acetonitrile at 298 K

geometry. Yet, the kinetics of fluorescence relaxation (Fig. 4) clearly shows a presence of delayed component which could arrive if we take into account a presence of a second state in thermal equilibrium with the emitting state. Thus, we applied a theoretical two excited state model in order to find dynamic parameters of the relaxation decay curve.

The analysis of fitting result indicates that probably, the planar excited conformation of the dye formed immediately after excitation transforms to a new geometrically 'locked' (by twisting on acceptor side) state with a rate of $8.33 \times 10^{-9}\,s^{-1}$ (corresponding to the theoretical relaxation time of 120 ps in fit). Once the thermodynamic equilibrium is established, the 'locked' state restitutes the population of the planar state and delayed relaxation kinetics with slower time constant of 270 ps is observed. Taking into account the radiative decay with the time constant of 4.3 ns ($0.24 \times 10^{-9}\,s^{-1}$) obtained from the exited state lifetime and fluorescence quantum yield we can estimate the non-radiative relaxation rate of the molecular system $K_{nr} = 2.71 \times 10^{-9}\,s^{-1}$.

It should be pointed out that the hypsochromic shifts in the absorption spectra of the complexes **1**–**4** were found to be substantially larger than those in the emission spectra. These phenomena were described in sufficient detail in the literature and are associated with the photoinduced charge transfer in excited states which reduces the electron density on the nitrogen atom of the crown.[40,43] This nitrogen atom becomes a non-coordinating atom positively polarized which repulses the cation. Thus, the Fig. 5 clearly indicates such phenomenon. Time-resolved fluorescence experiment with acetonitrile solution of the complex $(\mathbf{4})_1 \cdot (Hg^{2+})_2$ show wavelength-dependent decays. Biexponential decay with a 52 and 155 ps lifetime is found in the red-edge part of the fluorescence spectrum, whereas an extra short component of 6.5 ps is found in the short-wavelength edge. These results further indicate the presence of three emitting species after excitation of the complex. The very first process relaxing at 6.5 ps most probably is associated with the fast retiring movement of Hg cation from amine nitrogen. During this process, one can observe an apparent shift of the time-resolved fluorescence to the red side of spectrum of Fig. 5. We attribute the species with a lifetime of about 52 ps and 155 ps to the monocomplex $(\mathbf{4})_1 \cdot (Hg^{2+})_1$, a complex in which one Hg^{2+} cation is no longer in interaction with the nitrogen of the one azathiacrown ether fragment. As it was mentioned above, appearance of long lifetime component 155 ps in complex $(\mathbf{4})_1 \cdot (Hg^{2+})_2$ as compared with free ligand **4** after releasing of one Hg^{2+} cation from one azathiacrown ether fragment could be due to intramolecular charge transfer from non-complexed N-atom to the extended acceptor which already contained Hg^{2+} in another crown ether fragment or due to formation of geometrically 'locked' (by twisting on acceptor side) state.

Conclusion

In this work the synthesis and detailed investigation of optical characteristics and complexation ability of phenylazathiacrown ether dyes **1**–**4** with Hg^{2+}, Ag^+, Cu^{2+} cations was done. It was demonstrated that various mutual dispositions of styryl

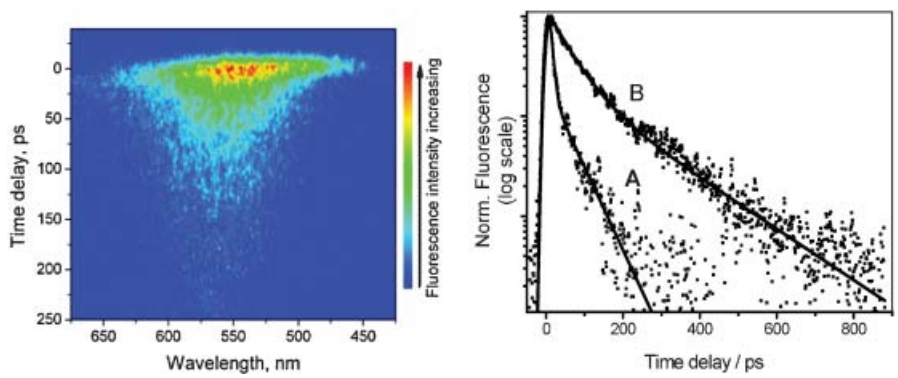

Figure 5. Time-spectrum-resolved fluorescence map (left) and fluorescence decay curves at 475 nm (A) and 600 nm (B) (right) for the complex $(\mathbf{4})_1 \cdot (Hg^{2+})_2$ excited at 360 nm in acetonitrile at 298 K

fragments in pyridinium residue results in the substantial difference in optical properties. It was also shown that dyes **1**–**4** are sensitive to the presence of H^+ and Hg^{2+}, Ag^+, Cu^{2+} cations. The response of compounds **1**–**4** is useful both in absorption and emission spectroscopy: the strong wavelength shifts observed in the presence of cations make the dyes suitable for dual wavelength analysis in self-calibrating measurements. The interaction strength between ligands and cations was measured. Evidence was given for the occurrence of two stoichiometries: LM and LM_2. The most stable complexes were formed with mercury. Due to simple model of complex formation, the reliable correlation between the concentration of metal cations in solution and value of optical response of dyes **1**–**4** can be obtained. So compounds can be considered as probe designed with the purpose to measure cation concentration in different kind of cationic analysis.

EXPERIMENTAL

Materials

Anhydrous MeCN, $Hg(ClO_4)_2$, $AgClO_4$, $Cu(ClO_4)_2$ (Aldrich) were used as received.

Solutions of dye **1**–**4** were prepared and used in redlight.

Synthesis and NMR study

^{1}H NMR spectra were recorded on a Bruker DRX500 instrument (500.13 MHz) and a Bruker DPX400 instrument (400.16 MHz) by means of a 5 mm direct QNP 1H/X probe with gradient capabilities.

*General synthetic route for **1**–**4***

Mixture contained 0.32 mmol of corresponded tosylates of dimethyl pyridinium (or trimethyl pyridinium) and 0.32 mmol (or 0.64 mmol for synthesis **3**, **4**) 4-(1,4-dioxa-7,13-dithia-10-azacyclopentadecan-10-yl)benzaldehyde, 0.1 ml of pyrrolidine and 3 ml *n*-BuOH was refluxed during 30 min. Solvent was evaporated and residue was washed with three portions (10 ml) of boiled benzene. Obtained precipitation was dissolved in dry MeOH and 0.32 mmol $NaClO_4$ was added. Orange–red precipitation was filtered-off and washed with Et_2O.

*10-(4-{(E)-2-[1-methyl-1-(perchloryloxy)-1l5-pyridin-4-yl]vinyl}phenyl)-1,4-dioxa-7,13-dithia-10-azacyclopentadecane (**1**)*

Yield 71%. M.p. 232 °C.^{1}H NMR (400 MHz, DMSO-d_6, 25 °C): δ 2.74 (t, 4 H, C(3)—H, C(14)—H, $^3J_{H,H} = 5.2$ Hz), 2.83 (t, 4 H, C(5)—H, C(12)—H, $^3J_{H,H} = 7.0$ Hz), 3.57 (s, 4 H, C(8)—H, C(9)—H), 3.69 (m, 8 H, C(2)—H, C(6)—H, C(11)—H, C(15)—H), 4.16 (s, 3 H, $C\underline{H}_3$), 6.71 (d, 2 H, C(17)—H, C(21)—H, $^3J_{H,H} = 8.3$ Hz), 7.14 (d, 1 H, C(b)—H, $^3J_{H,H} = 16.3$ Hz), 7.58 (d, 2 H, C(18)—H, C(20)—H, $^3J_{H,H} = 8.3$ Hz), 7.88 (d, 1H, C(a)—H, $^3J_{H,H} = 16.3$ Hz), 8.03 (d, 2H, C(3′)—H, C(5′)—H, $^3J_{H,H} = 6.3$ Hz), 8.66 (d, 2H, C(2′)—H, C(6′)—H, $^3J_{H,H} = 6.3$ Hz). $C_{24}H_{33}ClN_2O_6S_2$. Calcd. C 52.88, H 6.1, N 5.14; Found C 53.04, H 5.98, N 5.06%. ESI-MS **1** in MeCN *m/z*: 445.2 [$\mathbf{1}^+$].

*10-(4-{2-[1-Methyl-1-(perchloryloxy)-pyridin-2-yl]vinyl}phenyl)-1,4-dioxa-7,13-dithia-10-azacyclopentadecane (**2**)*

Yield 63%. M.p. 165–167 °C.^{1}H NMR (400 MHz, DMSO-d_6, 25 °C): δ 2.74 (t, 4 H, C(3)—H, C(14)—H, $^3J_{H,H} = 5.2$ Hz), 2.83 (t, 4 H, C(5)—H, C(12)—H, $^3J_{H,H} = 7.0$ Hz), 3.57 (s, 4 H, C(8)—H, C(9)—H), 3.69 (m, 8 H, C(2)—H, C(6)—H, C(11)—H, C(15)—H), 4.27 (s, 3 H, $C\underline{H}_3$), 6.72 (d, 2 H, C(17)—H, C(21)—H, $^3J_{H,H} = 8.6$ Hz), 7.12 (d, 2 H, C(b)—H, $^3J_{H,H} = 15.8$ Hz), 7.69 (d, 2 H, C(18)—H, C(20)—H, $^3J_{H,H} = 8.6$ Hz), 7.70 (t, 1 H, C(4′)—H, $^3J_{H,H} = 8.5$ Hz), 7.88 (d, 1 H, C(a)—H, $^3J_{H,H} = 15.8$ Hz), 8.33 (t, 1 H, C(5′)—H, $^3J_{H,H} = 7.3$ Hz), 8.42 (d, 1 H, C(3′)—H, $^3J_{H,H} = 8.5$ Hz), 8.73 (d, 1 H, C(6′)—H, $^3J_{H,H} = 7.3$ Hz)). $C_{24}H_{33}ClN_2O_6S_2$. Calcd. C 52.88, H 6.1, N 5.14; Found C 52.97, H 6.17, N 5.08%. ESI-MS **2** in MeCN *m/z*: 445.2 [$\mathbf{2}^+$].

*10,10′-{[1-Methyl-1-(perchloryloxy)-pyridine-2,4-diyl]bis[(E) ethene-2,1-diyl-4,1-phenylene]}bis-1,4-dioxa-7,13-dithia-10-azacyclopentadecane (**3**)*

Yield 68%. M.p. 257 °C.^{1}H NMR (400 MHz, DMSO-d_6, 25°C): δ 2.75 (t, 8 H, C(3)—H, C(3′)—H, C(14)—H, C(14′)—H, $^3J_{H,H} = 5.2$ Hz), 2.84 (t, 8 H, C(5)—H, C(5′)—H, C(12)—H, C(12′)—H, $^3J_{H,H} = 7.0$ Hz), 3.58 (s, 8 H, C(8)—H, C(8′)—H, C(9)—H, C(9′)—H), 3.69 (m, 16 H, C(2)—H, C(2′)—H, C(6)—H, C(6′)—H, C(11)—H, C(11′)—H, C(15)—H, C(15′)—H), 4.13 (s, 3 H, $C\underline{H}_3$), 6.72 (d, 4 H, C(17)—H, C(17′)—H, C(21)—H, C(21′)—H, $^3J_{H,H} = 8.4$ Hz), 7.09 (d, 1 H, C(b′)—H, $^3J_{H,H} = 16.2$ Hz), 7.21 (d, 1 H, C(b)—H, $^3J_{H,H} = 15.7$ Hz), 7.55 (d, 2 H, C(18′)—H, C(20′)—H, $^3J_{H,H} = 8.4$ Hz), 7.68 (d, 2 H, C(18)—H, C(20)—H, $^3J_{H,H} = 8.4$ Hz), 7.77 (d,1 H, C(5″)—H, $^3J_{H,H} = 6.9$ Hz), 7.83 (d, 1H, C(a)—H, $^3J_{H,H} = 15.7$ Hz), 7.83 (d, 1 H, C(a)—H, $^3J_{H,H} = 16.2$ Hz), 8.33 (s, 1 H, C(3″)—H), 8.51 (d, 1 H, C(6″)—H, $^3J_{H,H} = 6.9$ Hz). $C_{42}H_{58}ClN_3O_8S_2$. Calcd 56.26, H 6.52, N 4.69; found C 56.21, H 6.48, N 4.70%. ESI-MS **3** in MeCN *m/z*: 796.3 [$\mathbf{3}^+$].

*10,10′-{[1-Methyl-1-(perchloryloxy)-pyridine-2,6-diyl]bis[(E) ethene-2,1-diyl-4,1-phenylene]}bis-1,4-dioxa-7,13-dithia-10-azacyclopentadecane (**4**)*

Yield 65%. M.p. 220–225 °C.^{1}H NMR (400 MHz, DMSO-d_6, 25 °C): δ 2.75 (t, 8 H, C(3)—H, C(3′)—H, C(14)—H, C(14′)—H, $^3J_{H,H} = 5.2$ Hz), 2.84 (t, 8 H, C(5)—H, C(5′)—H, C(12)—H, C(12′)—H, $^3J_{H,H} = 7.0$ Hz), 3.58 (s, 8 H, C(8)—H, C(8′)—H, C(9)—H, C(9′)—H), 3.69 (m, 16 H, C(2)—H, C(2′)—H, C(6)—H, C(6′)—H, C(11)—H, C(11′)—H, C(15)—H, C(15′)—H), 4.17 (s, 3 H, $C\underline{H}_3$), 6.71 (d, 4 H, C(17)—H, C(17′)—H, C(21)—H, C(21′)—H, $^3J_{H,H} = 8.6$ Hz), 7.28 (d, 2 H, C(b)—H, C(b′)—H, $^3J_{H,H} = 15.7$ Hz), 7.65 (d, 2H, C(a)—H, C(a′)—H, $^3J_{H,H} = 15.7$ Hz), 7.67 (d, 4 H, C(18)—H, C(18′)—H, C(20)—H, C(20′)—H, $^3J = 8.6$ Hz), 8.07 (d, 2 H, C(3‴;)—H, C(5‴;)—H, $^3J_{H,H} = 7.8$ Hz), 8.20 (d, 1 H, C(4‴;)—H, $^3J_{H,H} = 7.8$ Hz).$C_{42}H_{58}ClN_3O_8S_2$. Calcd 56.26, H 6.52, N 4.69; Found C 56.34, H 6.56, N 4.66%. ESI-MS **4** in MeCN, *m/z*: 796.3 [$\mathbf{4}^+$].

UV–visible spectra

Preparation of solutions and all experiments were carried out in red light. The fluorescence quantum yield measurements were provided using Specord-M40 and Varian–Cary spectrophotometers and a FluoroLog (Jobin Yvon) spectrofluorimeter. All measured fluorescence spectra were corrected for the non-uniformity of detector spectral sensitivity. 9,10-Diphenylanthracene in cyclohexane ($\Phi^{fl} = 0.9$, according to Hamai and Hirayama[36]) was used.

Equilibrium constant determination

Complex formation of **1** with $AgClO_4$, $Cu(ClO_4)_2$, $Hg(ClO_4)_2$ or $HClO_4$ in acetonitrile at 20 ± 1 °C was studied by spectrophotometric titration. The ratio of **1**–**4** to $AgClO_4$, $Cu(ClO_4)_2$, $Hg(ClO_4)_2$ and $HClO_4$ was varied by adding aliquots of a solution

containing known concentrations of **1**–**4** and of corresponding salt or acid to a solution of **1**–**4** alone of the same concentration. The absorption spectrum of each solution was recorded and the stability constants of the complexes were determined using the HYPERQUAD programme.

Time-resolved fluorescence studies

The fluorescence excitation light pulses were obtained by frequency doubling and tripling of a Ti: sapphire femtosecond laser system (Femtopower Compact Pro) output. All excited state lifetimes were obtained using depolarized excitation light. The highest pulse energies used to excite fluorescence did not exceed 100 nJ and the average power of excitation beam was 0.1 mW at a pulse repetition rate of 1 kHz focused into a spot with a diameter of 0.1 mm in the 10 mm long fused silica cell. The fluorescence emitted in the forward direction was collected by reflective optics and focused with a spherical mirror onto the input slit of a spectrograph (Chromex 250) coupled to a streak camera (Hamamatsu 5680 equipped with a fast single sweep unit M5676, temporal resolution 2 ps). The convolution of a rectangular streak camera slit in the sweep range of 250 ps with an electronic jitter of the streak camera trigger pulse provided a Gaussian (over 4 decades) temporal apparatus function with a FWHM of 20 ps. The fluorescence kinetics were later fitted by using the Levenberg–Marquardt least-squares curve-fitting method using a solution of the differential equation describing the evolution in time of a single excited state and neglecting depopulation of the ground state:

$$\frac{dI(t)}{dt} = \text{Gauss}(t0, \Delta t, A) - \frac{I(t)}{\tau}$$

where $I(t)$ is the fluorescence intensity, Gauss is the Gaussian profile of the excitation pulse, where $t0$ stands for the excitation pulse arrival delay, Δt is the excitation pulse width and A is the amplitude. The parameter τ represents the lifetime of the excited state. The initial condition for the equation is $I(-\infty) = 0$. Typically, the fit shows a χ^2-value better than 10^{-4} and a correlation coefficient $R > 0.999$. The uncertainty of the lifetime was better than 0.1 ps. Routinely, the fluorescence accumulation time in our 35 measurements did not exceed 90 s.

In some cases, the kinetics were fitted using a system of differential equations describing the evolution in time of two excited populations in precursor–successor relationship:

$$\frac{dN_1(t)}{dt} = \text{Gauss}(t0, \Delta t, A) - \frac{N_1(t)}{\tau_1}$$
$$\frac{dN_2(t)}{dt} = \frac{N_1(t)}{\tau_1} - \frac{N_2(t)}{\tau_2}$$

where N_1 and N_2 represent the population of two excited state population, τ_1 and τ_2 are the lifetimes of corresponding populations. Other parameters as well as initial conditions are similarly defined as described above.

Acknowledgements

This research was sponsored by PICS, contract/grant number: 3904; RFBR, contract/grant numbers: 05-03-33201; The federal target programme 'Researches in priority directions of development of a scientifically technological complex of Russian Federation for 2007–2012' (State contracts 02.513.11.3133, 02.513.11.3208); and Ministry of Science and Education, Grant supporting for talented students, PhD students and young scientists of M. V. Lomonosov Moscow State University and Russian Science Support Foundation.

REFERENCES

[1] S. Fery-Forgues, F. Al-Ali, *J. Photochem. Photobiol. C Photochem. Rev.* **2004**, *5*, 139–153.
[2] H. Sakamoto, K. Kimura, Y. Koseki, M. Matsuo, T. Shono, *J. Org. Chem.* **1986**, *51*, 4974–4979.
[3] S. Sinkai, T. Ogawa, Y. Kusano, O. Manabe, K. Kikukawa, T. Goto, T. Matsuda, *J. Am. Chem. Soc.* **1982**, *104*, 1960–1967.
[4] Y. H. Cho, S. G. Rha, S. K. Chang, T. D. Chung, K. C. Cho, H. J. Kim, *Inclusion Phenom. Mol. Recognit. Chem.* **1998**, *31*, 119–129.
[5] J. D. Lamb, J. J. Christensen, J. L. Oscarson, B. L. Nielsen, B. W. Asay, R. M. Izatt, *J. Am. Chem. Soc.* **1980**, *102*, 6820–6824.
[6] A. M. Costero, C. Andreu, M. Pitarch, *Tetrahedron* **1996**, *52*, 3683–3686.
[7] S. Flink, B. A. Boukamp, A. F. Berg, F. C. Veggel, D. N. Reinhoudt, *J. Am. Chem. Soc.* **1998**, *120*, 4652–4657.
[8] S. Flink, F. C. Veggel, D. N. Reinhoudt, *J. Phys. Chem. B.* **1999**, *103*, 6515–6520.
[9] S. Y. Lin, S. W. Liu, C. M. Lin, C. H. Chen, *Anal. Chem.* **2002**, *74*, 330–335.
[10] C. Mingotaud, B. Agricole, C. Jego, *J. Phys. Chem.* **1995**, *99*, 17068–17070.
[11] S. Pfeiffer, C. Mingotaud, C. Garrigou-Lagrange, P. Delhaes, A. Sastre, T. Torres, *Langmuir* **1995**, *11*, 2705–2712.
[12] P. F. Chu, J. Y. Zhang, F. J. Zeng, L. Jiang, Q. X. Lin, H. S. Xu, *Kexue Tongbao (Foreign Lang. Ed.)* **1983**, *28*, 762.
[13] P. F. Chu, J. Y. Zhang, F. J. Zeng, L. Jiang, Q. X. Lin, H. S. Xu, *Chem. Abstr.* **1984**, *100*, 28088a.
[14] Q. X. Lin, H. S. Xu, F. Kezue, *Yu Huaxue Yanjiu* **1983**, *3*, 69–673.
[15] Q. X. Lin, H. S. Xu, F. Kezue, *Chem. Abstr.* **1983**, *99*, 141521b.
[16] H. An, J. S. Bradshaw, R. M. Izatt, Z. Yan, *Chem. Rev.* **1994**, *94*, 939–991.
[17] N. Marcotte, S. Fery-Forgues, D. Lavabre, S. Marguet, V. G. Pivovarenko, *J. Phys. Chem. A* **1999**, *103*, 3163–3170.
[18] E. V. Tulyakova, O. A. Fedorova, Y. V. Fedorov, G. Jonusauskas, L. G. Kuzrmina, J. Howard, A. V. Anisimov, *Russ. Chem. Bull.* **2007**, *56*, 513–526.
[19] S. H. Kawai, *Tetrahedron Lett.* **1998**, *39*, 4445–4448.
[20] M. E. Padilla-Tosta, J. M. Lloris, R. Martenez-Manez, M. D. Marcos, M. A. Miranda, T. Pardo, F. Sancenon, J. Soto, *Eur. J. Inorg. Chem.* **2001**, 1475–1482.
[21] P. D. Beer, S. W. Dent, N. C. Fletcher, T. J. Wear, *Polyhedron* **1996**, *15*, 2983–2996.
[22] S. Das, K. G. Thomas, K. J. Thomas, M. V. George, I. Bedja, P. V. Kamat, *Anal. Proc.* **1995**, *32*, 213–215.
[23] S. H. Kim, S. K. Han, S. H. Park, C. M. Yoon, S. R. Keum, *Dyes Pigm.* **1999**, *43*, 21–25.
[24] A. O. Doroshenko, A. V. Grigorovich, E. A. Posokhov, V. G. Pivovarenko, A. P. Demchenko, A. D. Sheiko, *Russ. Chem. Bull.* **2001**, *50*, 404.
[25] N. Marcotte, S. Fery-Forgues, *J. Photochem. Photobiol. A Chem.* **2000**, *130*, 133–138.
[26] H. Wang, R. Helgeson, B. Ma, F. Wudl, *J. Org. Chem.* **2000**, *65*, 5862–5867.
[27] A. I. Kipriyanov, *Tsvet and Stroenie Cyaninovix Krasitelei*. Naukova Dumka, Kiev, **1979**, 392–397.
[28] A. I. Kipriyanov, G. G. Dyadyushka, *Ukr. Chem. J.* **1969**, *35*, 608–609.
[29] X. Cao, R. W. Tolbert, J. L. McHale, W. D. Edwards, *J. Phys. Chem. A* **1998**, *102*, 2739–2748.
[30] B. Strehmel, H. Seifert, W. Rettig, *J. Phys. Chem. B* **1997**, *101*, 2232–2243.
[31] O. A. Fedorova, Y. V. Fedorov, A. I. Vedernikov, S. P. Gromov, O. V. Yescheulova, M. V. Alfimov, M. Woerner, S. Bossmann, A. Braun, J. Saltiel, *J. Phys. Chem. A* **2002**, *106*, 6213–6222.
[32] M. Izatt, G. Wu, W. Jiang, N. K. Dall, *Inorg. Chem.* **1990**, *29*, 3828–3832.
[33] M. V. Alfimov, A. V. Churakov, Y. V. Fedorov, O. A. Fedorova, S. P. Gromov, R. E. Hester, J. A. K. Howard, L. G. Kuz'mina, I. K. Lednev, *J. Chem. Soc. Perkin Trans. 2* **1997**, *11*, 2249–2256.

[34] W. Grochala, A. Jagielska, C. Wozaniak, A. Wieeckowska, R. Bilewicz, B. Korybut-Daszkiewicz, J. Bukowska, L. Piela, *J. Phys. Org. Chem.* **2001**, *14*, 63–73.
[35] K. Rurack, J. L. Bricks, G. Reck, R. Radeglia, U. Resch-Genger, *J. Phys. Chem. A* **2000**, *104*, 3087–3109.
[36] V. A. Livshits, A. M. Pronin, V. V. Samoshin, S. P. Gromov, M. V. Alfimov, *Russ. Chem. Bull.* **1994**, *43*, 1827–1833.
[37] T. E. Jones, D. B. Rorabacher, L. A. Ochrymowycz, *J. Am. Chem. Soc.* **1975**, *97*, 7485–7486.
[38] A. R. Amundsen, J. Whelan, B. Bosnich, *J. Am. Chem. Soc.* **1977**, *99*, 6730–6739.
[39] Y. Zhang, J. Li, Q. Su, Q. Wang, X. Wu, *J. Mol. Struct.* **2000**, *516*, 231–236.
[40] R. Mathevet, G. Jonusauskas, C. Rulliere, *J. Phys. Chem.* **1995**, *99*, 15709–15713.
[41] B. Valeur, *Molecular Fluorescence: Principles and Application*, C Vol. 10. Willey, New York, **2001**, 299–305.
[42] M. J. Meer, H. Zhang, W. Rettig, M. Glasbeek, *Chem. Phys. Lett.* **2000**, *320*, 673–680.
[43] M. Martin, P. Plaza, Y. Meyer, F. Badaoui, J. Bourson, J. P. Lefévre, B. Valeur, *J. Phys. Chem.* **1996**, *100*, 6879–6888.